Infrared Spectroscopic Study of $CH_3\cdots O{=}C$ Interaction during Poly(L-lactide)/Poly(D-lactide) Stereocomplex Formation

Jianming Zhang,[†] Harumi Sato,[†] Hideto Tsuji,[‡] Isao Noda,[§] and Yukihiro Ozaki*,[†]

Department of Chemistry, School of Science and Technology, Kwansei-Gakuin University, Gakuen, Sanda 669-1337, Japan; Department of Ecological Engineering, Faculty of Engineering, Toyohashi University of Technology, Tempaku-cho, Toyohashi, Aichi 441-8580, Japan; and The Procter & Gamble Company, 8611 Beckett Road, West Chester, Ohio 45069

Received October 14, 2004; Revised Manuscript Received December 6, 2004

ABSTRACT: The nature of the "peculiarly strong" interaction between the poly(L-lactide) (PLLA) and poly(D-lactide) (PDLA) chains was investigated by real time infrared spectroscopy during the isothermal melt crystallization process of the PLLA/PDLA stereocomplex. A very small low-frequency shift (about 1 cm^{-1}) of $\nu_{as}(CH_3)$ and a larger low-frequency shift (about 5 cm^{-1}) of $\nu(C{=}O)$ were observed. The typical butterfly pattern in the two-dimensional (2D) asynchronous correlation spectrum and the second-derivative spectra reveal that there is a "peak shift" for $\nu(C{=}O)$. The red shifts of the stretching vibration modes of the methyl and carbonyl groups suggest that the interaction between the PLLA/PDLA stereocomplex is ascribed to $CH_3\cdots O{=}C$ hydrogen bonding. Another interesting result is that the peak shift of the $\nu(C{=}O)$ band already occurs in the induction period, which indicates that the $CH_3\cdots O{=}C$ interaction is the driving force for forming the racemic nucleation of the PLLA/PDLA stereocomplex. Moreover, the 2D correlation analysis indicates that the structural adjustment of the CH_3 group occurs prior to that of the C−O−C backbone during the stereocomplexation process of PLLA/PDLA. The $CH_3\cdots O{=}C$ interaction may be the reason for this sequence of structural changes.

1. Introduction

Among the family of biodegradable aliphatic polyesters, poly(lactic acid) (PLA) ($[CH(CH_3)COO]_n-$) has been attracting much attention, because it is producible from renewable resources, such as starch, and has very low or no toxicity and high mechanical performance comparable to those of polyethylene and polystyrene.[1] Due to the presence of a heteroatom in the main chain (which has a chemical polarity), PLA is a genuine chiral polymer, the two enantiomers of which have been synthesized.[2] Crystalline poly(L-lactide) (PLLA) forms left-handed helices, while crystalline poly(D-lactide) (PDLA) adopts right-handed helices.[3] Since Ikada et al.[3] found a stereocomplex formation from equimolar mixtures of PLLA and PDLA in both melts and solutions, numerous studies have been performed on the formation and crystallization of the stereocomplex as well as its crystalline structure, morphology, and physical properties.[4−8] It has been found that the stereocomplex crystallizes in a triclinic unit cell to form a 3_1 helical conformation known as the β-form.[3−5] In contrast, the individual polyenantiomers crystallize either in a pseudoorthorhombic system with two 10_3 helices (known as the α-form)[9−11] or in a "distorted 3_1-helix α-form".[11] The β-form of PLLA can also be obtained by changing the conditions used to form fiber samples.[12,13] A new γ form produced through epitaxial crystallization was also recently described by Cartier et al.[14] Table 1 summarizes the crystalline structures, melting points, and preparation conditions of different crystalline forms acquired for the PLLA/PDLA stereocomplex and pure PLLA (or PDLA). Noticeablely, the physical properties of the PLLA/PDLA stereocomplex are markedly different from those of the individual homopolymers of PLA, for example, (1) higher thermal stability, having a melting temperature (230 °C) that is significantly higher than those of the enantiomeric α and β forms (180 and 170 °C, respectively), despite very similar or (for the β structure) even identical helix conformations[3,12,13] and (2) higher hydrolysis resistance compared with that of pure PLLA and PDLA even in the amorphous state.[15]

Obviously, the different helix structure is not the main reason for the high stability of the PLLA/PDLA stereocomplex. On the basis of the distinct physical properties of the PLLA/PDLA stereocomplex above, Tsuji et al.[15] speculated that there are peculiarly strong interactions between the left- and right-handed helices of PLLA and PDLA in the stereocomplex. By force field simulation of the stereocomplex unit cells and of their powder patterns, Brizzolara et al.[5] proposed that van der Waals interactions are formed between opposite oxygen atoms and hydrogen atoms, and such interactions cause the stabilization of the 3_1 helix and the higher melting point of the complex. However, experimental evidence which elucidates the exact nature of such "peculiar" interactions in the PLLA/PDLA stereocomplex is still lacking.

In the past decade, the importance of C−H···O interactions has been recognized not only in simple molecules but also in biological molecules such as nucleic acids,[16−18] proteins,[19,20] and carbohydrates.[21,22] The widespread occurrence of C−H···O interactions has made them an active topic of research from both theoretical[23−25] and experimental[23,26] perspectives. However, conclusive experimental evidence for C−H···O hydrogen bonding in biological macromolecules is notoriously difficult to obtain, because the weak C−H···O interactions usually coexist with other stronger hydrogen bonds, making the contribution from the C−H···O interactions difficult to distinguish. Nevertheless, it has

* To whom correspondence should be addressed. Fax: +81-79-565-9077. E-mail: ozaki@ksc.kwansei.ac.jp.
† Kwansei-Gakuin University.
‡ Toyohashi University of Technology.
§ The Procter & Gamble Co.

10.1021/ma047872w CCC: $30.25
Published on Web 02/03/2005

Table 1. Comparison of the Crystalline Structure, Melting Point, and Preparation Conditions of Different Crystalline Forms for the PLLA/PDLA Stereocomplex and Pure PLLA (or PDLA)[3−5,9−14]

	crystalline form	unit cell	helical conformation	T_m (°C)	preparation conditions
PLLA (or PDLA)	α	pseudo-orthorhombic	10_3	∼180	solution or melt
	β	trigonal	3_1	∼170	high draw ratio and temperature
	γ	orthorhombic	3_2		epitaxial crystallization
PLLA/PDLA stereo-complex	β	triclinic	3_1	∼230	1:1 blend

been suggested that the C−H···O interactions play important functional and structural stabilization roles in biological systems.[23,27] PLA is a kind of polyester with simple molecular structure. There are no strong hydrogen bonds among the PLA chains, and only dipole−dipole interactions, weak C−H···O hydrogen bonds, and van der Waals interactions are expected. Therefore, it is a suitable model for investigating the weak C−H···O hydrogen bond.

On the basis of our previous studies on the spectral changes of pure PLLA during the isothermal crystallization processes by infrared and two-dimensional infrared correlation spectroscopy,[28,29] we explore in this study the structural dynamics and intermolecular interactions between the PLLA and PDLA chains during the melt crystallization of the PLLA/PDLA stereocomplex at 220 °C by real time IR spectroscopy. A very small low-frequency shift (about 1 cm^{-1}) of the $\nu_{as}(CH_3)$ band and a larger low-frequency shift (5 cm^{-1}) of the ν(C═O) band were observed with the formation of the PLLA/PDLA stereocomplex. These observations verify that the PLLA/PDLA stereocomplex forms the CH_3···O═C intermolecular interaction between the PLLA and PDLA chains that is attributed to a C−H···O hydrogen bond. The relatively large peak shift of the C═O band already occurs in the induction period, indicating that the CH_3···O═C interaction is the driving force for forming the racemic nucleation of the PLLA/PDLA stereocomplex.

2. Experimental Section

2.1. Materials and Sample Preparation Procedures. The synthesis and purification of PLLA and PDLA samples (PLLA, weight-average molar mass (M_w) = 150000 g mol^{-1} and M_w/number-average molar mass (M_n) = 1.80; PDLA, M_w = 100000 g mol^{-1} and M_w/M_n = 1.85) used in this study were performed according to the procedures reported previously.[30] The blend films for studying the PLLA/PDLA stereocomplex formation were obtained by the following casting method. A chloroform solution with a concentration of 1 g/dL was separately prepared for PDLA and PLLA, and then, the solutions were admixed with each other under stirring. The mixing ratio of the solutions was fixed at a 1:1 volume ratio. The mixed solution was cast onto a KBr plate, and the solvent was allowed to evaporate at room temperature for approximately 1 h. The resulting films were dried in vacuo for another 24 h.

2.2. FTIR Spectroscopy. For the IR experiment of the melt crystallization process of the PLLA/PDLA stereocomplex, the KBr plate with the solution cast film was set on a homemade variable-temperature cell, which was placed in the sample compartment of a Nicholet Magna 870 spectrometer equipped with an MCT detector. The sample was first heated at 10 °C/min to 240 °C (about 10 °C above the melting point of the PLLA/PDLA stereocomplex) for 1 min to melt the polymer and completely erase the thermal history. Then, it was cooled at 5 °C/min to 220 °C for the isothermal melt crystallization. IR spectra of the specimen were collected with a 1 min interval during the annealing process. The spectra were obtained by co-adding 16 scans at a 2 cm^{-1} resolution.

2.3. 2D IR Correlation Analysis. Before the 2D correlation analysis was performed, the IR spectra were preprocessed to minimize the effect of baseline instabilities and other nonselective effects. The frequency regions of interest were truncated first and subjected to a linear baseline correction, followed by offsetting to the zero absorbance value. Ten spectra at an equal time interval in a certain wavenumber range were selected for the 2D correlation analysis, which was carried out by using the software 2D Pocha composed by D. Adachi (Kwansei-Gakuin University). The time-averaged 1D reference spectra are shown at the side and top of the 2D correlation maps for reference. In the 2D correlation maps, regions without dots indicate positive correlation intensities, while those with dots indicate negative correlation intensities.

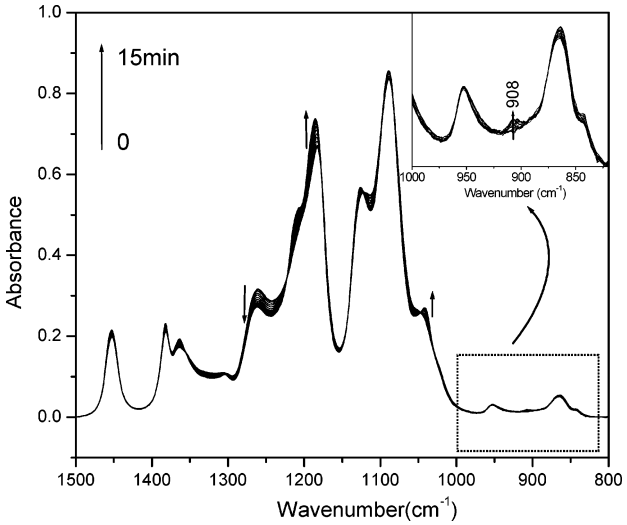

Figure 1. Time-dependent IR spectra in the range of 1500−1000 cm^{-1} collected during the melt crystallization process of the PLLA/PDLA stereocomplex at 220 °C.

3. Results and Discussion

3.1. Crystallization Kinetics of the PLLA/PDLA Stereocomplex. Usually, the melt crystallization of a PLLA and PDLA stereomixture is followed by the homocrystallization of PLLA and PDLA along with the crystallization of the stereocomplex. To avoid the effect of the homocrystallization, a crystallization temperature (T_c) at 220 °C, which is between the melting point of pure PLLA or PDLA (ca. 170 °C) and that of the PLLA/PDLA stereocomplex (ca. 230 °C), is chosen. Under such T_c, it is found that the crystallization rate is also suitable for real time FTIR measurement.

Figure 1 shows the time-dependent IR spectra in the range of 1500−800 cm^{-1} during the melt crystallization process of a PLLA/PDLA cast film at 220 °C. The enlarged spectra in the 1000−820 cm^{-1} region are shown in the inset of Figure 1. In the inset, one can clearly identify a new band at 908 cm^{-1}, which is the characteristic band of the PLLA/PDLA stereocomplex (β crystals).[31−33] On the other hand, the band at 923 cm^{-1}, which is assigned to the coupling of C−C backbone stretching with the CH_3 rocking mode and is sensitive to the 10_3 helix chain conformation of PLLA α crystals, is missing completely.[32,33] This observation provided the evidence that only the stereocomplex of PLLA/PDLA is formed and no homocrystallization of PLLA and PDLA

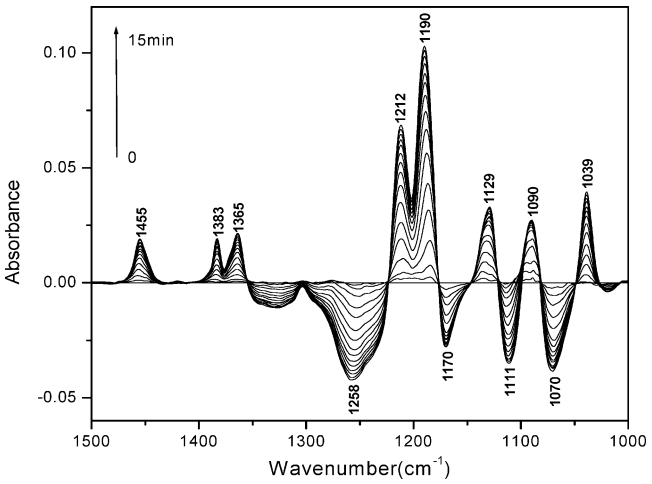

Figure 2. Time-dependent difference spectra calculated from the spectra shown in Figure 1.

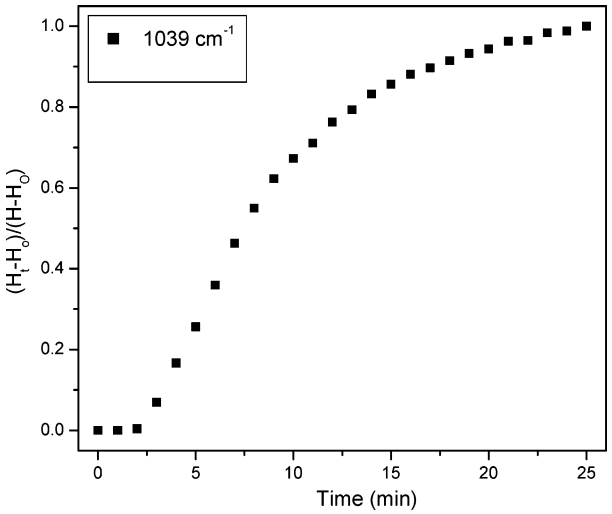

Figure 3. Normalized peak height of the crystalline sensitive band at 1039 cm^{-1} of the PLLA/PDLA stereocomplex as a function of crystallization time.

appears under such crystallization conditions. Since the intensity change in the characteristic band at 908 cm^{-1} is very small, it is difficult to derive the crystallization dynamics of the PLLA/PDLA stereocomplex at 220 °C by following its intensity change.

In the range of 1500−1000 cm^{-1}, bands are highly overlapped (Figure 1). To emphasize spectral changes and to relate the intensity changes of the bands to the crystallization kinetics, difference spectra were calculated by subtracting the initial (amorphous state) spectrum from the rest of the spectra in Figure 1. Figure 2 displays them. From the difference spectra, pronounced spectral changes during the melt crystallization of the PLLA/PDLA stereocomplex can be observed. In the range of 1500−1300 cm^{-1}, bands at 1455 and 1383 cm^{-1} are, respectively, due to CH_3 asymmetric and symmetric deformation modes and a band at 1365 cm^{-1} is associated with the combination of $\delta_s(CH_3)$ and $\delta(CH)$.[31] Relatively small intensity changes take place for these bands, while larger changes occur in the region from 1300 to 1000 cm^{-1}. In the range of 1300−1000 cm^{-1}, it is well-known that most of the bands are related to the C−O−C stretching vibration modes, although the precise assignments for the bands in this region are difficult. However, the band at 1039 cm^{-1} is well assigned to the stretching vibration of the $C-CH_3$ group,[31] and we noticed in our previous study[28,29] on the crystallization behaviors of PLLA that the stretching vibration of the $C-CH_3$ group appears at 1044 cm^{-1} in both the amorphous and semicrystalline samples. Therefore, it is rational to assign the new band at 1039 cm^{-1} in Figure 2 as a characteristic band of the PLLA/PDLA stereocomplex. Figure 3 plots the normalized peak height of the crystalline sensitive band at 1039 cm^{-1} in the difference spectra as a function of crystallization time at 220 °C. It can be seen from the plot that it takes about 25 min to complete the melt crystallization of the PLLA/PDLA stereocomplex at 220 °C, and that the induction time is about 2 min.

It has been well established that information about the specific order of spectral intensity changes taking place during spectral measurements can be derived from the analysis of a 2D asynchronous spectrum.[34,35] Figure 4 shows the synchronous $\Phi(\nu_1, \nu_2)$ and asynchronous $\Psi(\nu_1, \nu_2)$ 2D correlation spectrum in the range of 1500−1000 cm^{-1}, calculated from the difference spectra in Figure 2. In both 2D spectra, it can be seen that highly overlapped peaks are deconvoluted effectively by spreading the peaks along the second spectral dimension. An asynchronous spectrum represents sequential or successive changes of spectral intensities measured at ν_1 and ν_2. According to Noda's rule,[34,35] the sign of an

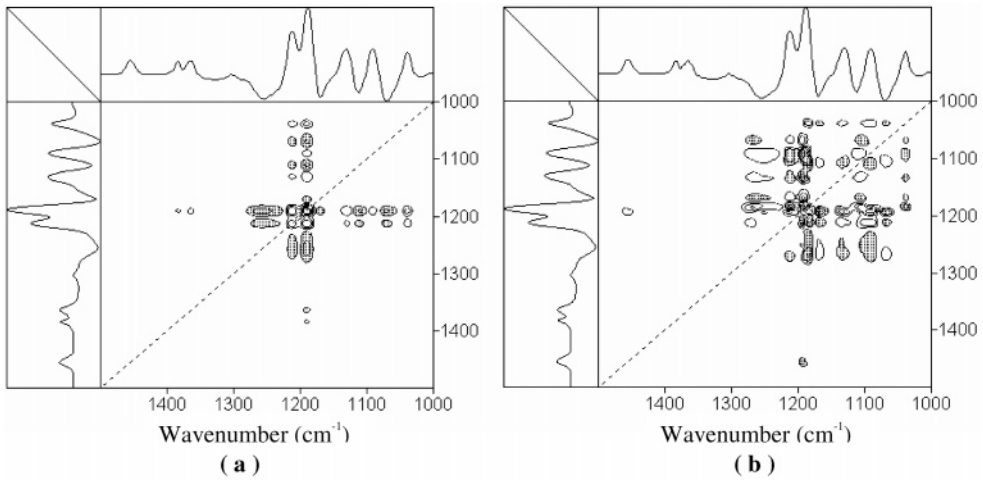

Figure 4. Synchronous and asynchronous correlation spectra of the PLLA/PDLA stereocomplex in the wavenumber region of 1500−1000 cm^{-1}, calculated from the spectra obtained during annealing at 220 °C.

asynchronous cross-peak becomes positive if the intensity change at ν_1 occurs predominantly before ν_2 in the sequential order of t. It becomes negative, on the other hand, if the change occurs after ν_2. This rule is, however, reversed if the corresponding synchronous intensity becomes negative, i.e., $\Phi(\nu_1, \nu_2) < 0$. The crystalline sensitive bands at 1455, 1190, 1129, and 1090 cm^{-1} show positive peaks in the difference spectra, indicating that the intensities of all these bands increase with the crystallization time. Accordingly, it is reasonable for them to share the positive synchronous cross-peaks ($\Phi(\nu_1, \nu_2) > 0$) in the synchronous spectrum (Figure 4a). In the corresponding asynchronous spectrum (Figure 4b), they have the following asynchronous cross-peaks: Ψ(1455, 1190), Ψ(1190, 1039), Ψ(1129, 1039), and Ψ(1090, 1039) > 0. These observations indicate that the sequential order of these crystalline sensitive bands is 1455 cm^{-1} > 1190 cm^{-1} and 1190, 1129, and 1090 cm^{-1} > 1039 cm^{-1}. As mentioned above, the bands at 1455 and 1039 cm^{-1} are assigned, respectively, to the CH_3 asymmetric deformation mode and C−CH_3 stretching vibration and the bands at 1190, 1129, and 1090 cm^{-1} are related to the C−O−C stretching vibration modes. Therefore, from the 2D correlation analysis, it seems that the change of the CH_3 group in PLLA or PDLA occurs prior to that of the C−O−C backbone, and that the structural adjustment of C−CH_3 is slower than that of the C−O−C backbone. During the cold crystallization processes of pure PLLA,[29] it is also found that the structural adjustment of the CH_3 group unambiguously precedes that of the ester group.

3.2. Intermolecular Interaction Between the C═O Group and the CH_3 Group. Because only CH_3 and C═O groups exist as the side groups in the PLLA or PDLA chain, it is very important to investigate changes in IR bands due to CH_3 and C═O groups for exploring the interchain interaction between the PLLA/PDLA chains. The spectral evolution in the C═O stretching region during the melt crystallization process of PLLA/PDLA stereocomplexation is shown in Figure 5a. Difference spectra calculated by subtracting the initial spectrum from the rest of the spectra in Figure 5a are displayed in Figure 5b. Obviously, during the crystallization process, the intensity of a positive peak at 1749 cm^{-1} increases gradually with time, while that of a negative peak at 1765 cm^{-1} decreases. It seems rational to assign the 1749 cm^{-1} band to ν(C═O) of the crystalline phase, and the 1765 cm^{-1} band to ν(C═O) of the amorphous phase. Recently, Bourque et al.[36] monitored the compression behavior of equimolar mixtures of PLLA and PDLA deposited on an air−water interface by the polarization modulation IR reflection absorption spectroscopy (PM-IRRAS) technique. They showed that these two components can be associated with the A and E modes of polylactide helices. However, in our transmission spectra, such positive and negative peaks in the difference spectra may be artificially generated by the crystallization-induced frequency shift or bandwidth narrowing of the actual IR spectra. Therefore, it is necessary to try other spectral analysis methods also. It is well established that 2D correlation spectroscopy has powerful deconvolution ability for highly overlapped bands.[35] Especially, an asynchronous correlation spectrum is sensitive to a small frequency shift or a bandwidth change. The asynchronous correlation spectrum calculated from the spectra in Figure 5a is depicted in Figure 5c. It is clear that a so-called

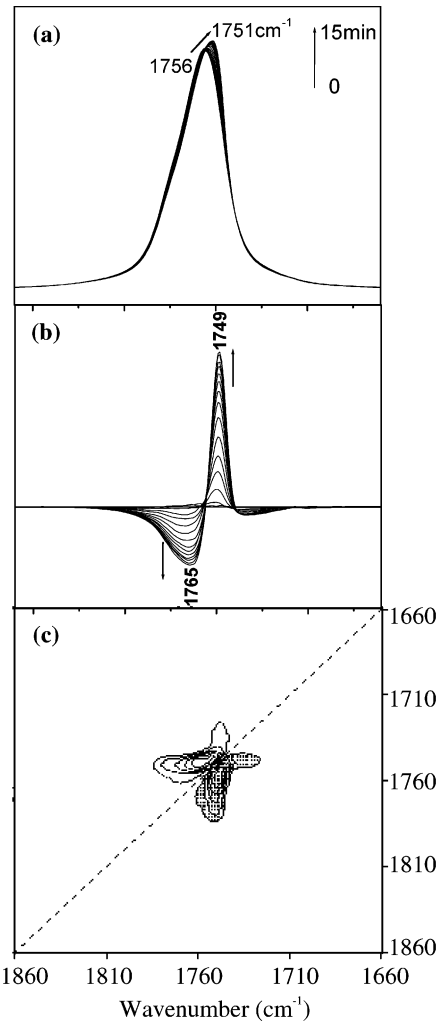

Figure 5. (a) Time-dependent IR spectra in the range of 1860−1660 cm^{-1} collected during the melt crystallization process of the PLLA/PDLA stereocomplex at 220 °C. (b) Corresponding difference spectra. (c) An asynchronous 2D IR correlation spectrum generated from (a).

"butterfly pattern" appears in the C═O stretching region. Usually, the appearance of a butterfly pattern in an asynchronous spectrum is attributed to a peak shift combined with the intensity changes.[37,38]

Figure 6a shows the second derivative of some of the spectra shown in Figure 5a. It can be seen that two bands (1776 and 1754 cm^{-1}) can be detected before the sterecomplex formation of PLLA/PDLA. With the transforming of the PLLA/PDLA sample from the amorphous state to the semicrystalline state, the band at 1754 cm^{-1} shifts to 1749 cm^{-1}, whereas the intensity and position of the band at 1776 cm^{-1} change little. A new band at 1760 cm^{-1} is clearly detected at the end of the stereocomplexation process. Obviously, the bands at 1760 and 1749 cm^{-1} are crystalline sensitive bands, which can be assigned to ν(C═O) of the amorphous and crystalline phases, respectively. The band at 1776 cm^{-1} is not a crystalline sensitive band, although it is difficult to make clear its origin.

One possible interpretation for the low-frequency shift of the crystalline band near 1749 cm^{-1} (Figure 6a) is the transition dipole coupling of the ester groups in the crystalline state. For polymer systems, a band splitting often occurs due to the dipole−dipole coupling when the molecules form an ordered structure.[39] It is well-known

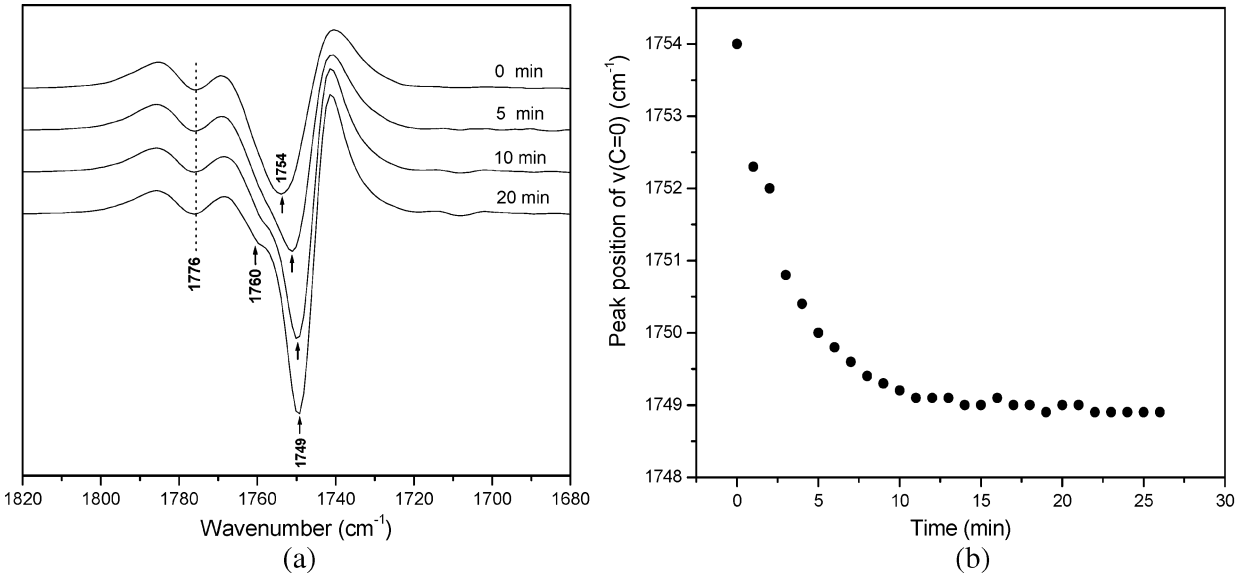

Figure 6. (a) Second derivatives of the spectra measured during the melt crystallization process of the PLLA/PDLA stereocomplex at 220 °C. The spectra were arranged with a 5 min interval from 0 to 20 min. (b) A plot of the peak position of the ν(C=O) band in the second derivatives of the spectra collected during the melt crystallization process of the PLLA/PDLA stereocomplex at 220 °C.

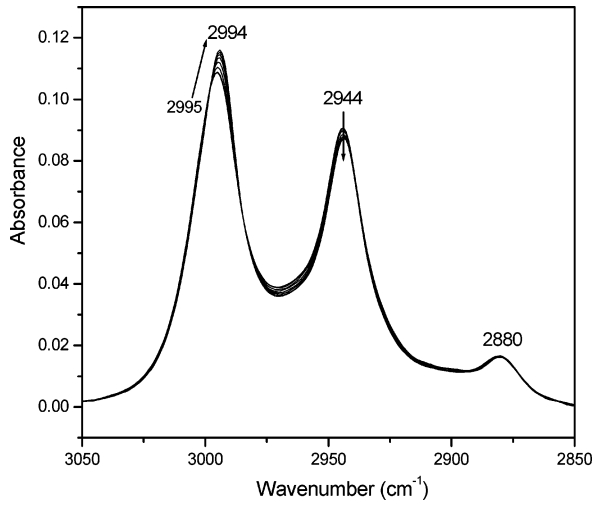

Figure 7. Temporal changes of the IR spectrum in the range of 3100−2850 cm^{-1} during the melt crystallization process of the PLLA/PDLA stereocomplex at 220 °C.

that such dipole−dipole interaction provides quite different spectral patterns for IR and Raman spectra. A comparison between the IR and Raman spectra of the PLLA/PDAL stereocomplex in the literature,[31] however, does not give any support for the existence of the dipole−dipole coupling. The other possibility is the intermolecular hydrogen bond interaction between the C=O and CH_3 groups. The low-frequency shift of the C=O stretching band is an important criterion for hydrogen bond formation of the C=O group.[40] Therefore, it is rational to speculate that there is a $CH_3\cdots O{=}C$ interaction between the PLLA/PDLA stereocomplex that is attributed to the hydrogen bond. This hydrogen bond must be weak because the low-frequency shift of the ν(C=O) band from the usual position for a free C=O group (1754 cm^{-1}) is so small.

To strengthen the above speculation, it is necessary to check the spectral changes in the C−H stretching region. Figure 7 illustrates the time-dependent spectral evolution in the C−H stretching region during the melt crystallization process of the PLLA/PDLA stereocomplex. Bands at 2995, 2944, and 2880 cm^{-1} are assigned, respectively, to the CH_3 asymmetric stretching, CH_2 stretching, and CH stretching modes. Obviously, the CH_3 asymmetric stretching mode shifts from 2995 to 2994 cm^{-1}, and its intensity also gradually increases with the formation of the PLLA/PDLA stereocomplex.

It is well-known that both the frequency shifts and intensities changes are characteristics for the specificity or magnitude of hydrogen bonds formed.[40] The frequency of an A−H stretching vibration is very sensitive to the H-bond formation and is generally shifted to a lower value as a consequence of the weakening of the A−H bond. The shift in the frequency of the A−H stretch is often used as the simplest spectroscopic criterion for the existence of H-bonding. Theoretical calculations have estimated the CH···O bonding interactions to be about 1−2 kcal/mol.[41−43] It has been reported that the racemic crystal of the PLLA/PDLA stereocomplex is formed by packing β form 3_1 helices of opposite absolute configuration alternatingly side by side. Brizzolara et al.[5] proposed that van der Waals interactions are formed between opposite oxygen atoms and hydrogen atoms. However, our observations for the frequency shifts of the ν(C=O) and $\nu_{as}(CH_3)$ bands indicate that the $CH_3\cdots O{=}C$ interaction is attributed to the hydrogen bond between the PLLA and PDLA chains. With the aforementioned shift of the C−H stretching band at hand, it is possible to calculate the $CH_3\cdots O{=}C$ bond strength using the empirical correlation between the frequency shift and H-bond strength proposed by Rozenberg and co-workers:[44] $\Delta G = 0.31\Delta\nu^{1/2}$ kcal/mol. Thus, the frequency shift of $\nu_{as}(CH_3)$ is indicative of a H-bond energy of $\Delta G = 0.31$ kcal/mol, which is lower than the value of the usual theoretical calculations mentioned above. This value demonstrates that the hydrogen bond strength between the C=O group and CH_3 group is weak. However, considering the long-chain property of a macromolecule, the overall contribution of such $CH_3\cdots O{=}C$ hydrogen bonds can account for the significant stability of the PDLA/PLLA stereocomplex. Moreover, the cooperatively of the hydrogen bonds can

magnify and improve the overall hydrogen bond effect between the PLLA and PDLA chains.

The distance between the oxygen atom of the C=O group and the hydrogen atom of one of the C−H bonds of the CH_3 group in a crystal unit is an important criterion for forming the hydrogen bond. However, we found that it is difficult to calculate the distance between them because of the lack of the reported atom coordinates of PLA. By comparing Figures 3 and 6b, it is found that the peak shift of the C=O band already occurs in the induction period, indicating that the CH_3··O=C interaction appears before the formation of the PLLA/PDLA crystal unit. However, for the individual polyenantiomer of PLA, it was found that the intermolecular dipole−dipole interaction of the CH_3 group appears during both the induction period and growth period of PLLA melt crystallization,[28] which provides direct evidence that the distorted 10_3 helix conformation of the PLLA chain in α crystals is due to the interchain interactions between CH_3 groups. Moreover, recently, Iwata et al.[45] found that the surface-grafted PLLA resists the adsorption of free PLLA chains but favors the adsorption of free PDLA chains. These observations show that the 3_1 helical chains of opposite absolute configuration of PLA tend to form the CH_3···O=C hydrogen bond, which is the driving force for forming the PLLA/PDLA stereocomplex.

4. Conclusion

In this study, we have investigated the melt crystallization behavior of a PLLA/PDLA blend film at 220 °C by means of IR spectroscopy. It has been verified that only the PLLA/PDLA stereocomplex is formed and no homocrystallization of PLLA and PDLA appears under such crystallization conditions. The crystallization dynamics of the PLLA/PDLA stereocomplex at 220 °C has been derived by monitoring the intensity changes in the C−CH_3 stretching band at 1039 cm^{-1} as a function of crystallization time. From the 2D correlation analysis, it has been found that the change of the CH_3 group in PLLA or PDLA occurs prior to the conformational adjustment of the C−O−C backbone, and that the structural evolution of C−CH_3 is slower than that of the C−O−C backbone. Of particular importance is that a very small low-frequency shift (about 1 cm^{-1}) of the ν_{as}-(CH_3) band and a larger low-frequency shift (5 cm^{-1}) of the ν(C=O) band were observed. These observations suggest that the CH_3···O=C among the PLLA/PDLA stereocomplex is attributed to the weak H-bond and that the energy of the H-bond is about Δ0.31 kcal/mol, which is lower than the value of the theoretical calculations. Moreover, it has been noted that the peak shift of the C=O band already occurs in the induction period, which indicates that the CH_3···O=C hydrogen bond is formed before the formation of the regular crystal structure of the PLLA/PDLA sterecomplex. In other words, the CH_3··O=C interaction among the β form 3_1 helices of opposite absolute configuration of PLA is the driving force for forming the racemic nucleation of the PLLA/PDLA stereocomplex. This situation is obviously different from that in the crystallization behavior of pure PLLA, in which the dipole−dipole intermolecular interaction of the CH_3 group among the 10_3 helices of the same absolute chain configuration appears in the induction period.[28] We have speculated that the CH_3···O=C interaction is also the reason the change of the CH_3 group occurs prior to that of the C−O−C backbone during the sterecomplex process of PLLA/PDLA.

Acknowledgment. The encouragement and support of Professor Dr. Yoshito Ikada, Suzuka University of Medical Science, for this study are greatly appreciated. J.Z. thanks the Japan Society for the Promotion of Science (JSPS) for financial support.

References and Notes

(1) Ikada, Y.; Tsuji, H. *Macromol. Rapid Commun*. **2000**, *21*, 117−132
(2) DeSantis, P.; Kovacs, A. J. *Biopolymers* **1968**, *6*, 299−306.
(3) Ikada, Y.; Jamshidi, K.; Tsuji, H.; Hyon, S.-H. *Macromolecules* **1987**, *20*, 904−906.
(4) Okihara, T.; Tsuji, M.; Kawaguchi, A.; Katayama, K.-I.; Tsuji, H.; Hyon, S.-H.; Ikada, Y. *J. Macromol. Sci., Phys.* **1991**, *B30*, 119−140.
(5) Brizzolara, D.; Cantow, H.-J.; Diederichs, K.; Keller, E.; Domb, A. J. *Macromolecules* **1996**, *29*, 191−197.
(6) Tsuji, H. In *Recent Research Developments in Polymer Science*; Pandalai, S. G., Ed.; Transworld Research Network: Trivandrum, India, 2000; Vol. 4, pp 13−37.
(7) Tsuji, H. In *Polyesters 3 (Biopolymers, vol. 4)*; Doi, Y., Steinbuchel, A., Eds.; Wiley-VCH: Weinheim, Germany, 2002; Chapter 5, pp 129−177.
(8) Tsuji, H.; Tezuka, Y. *Biomacromolecules* **2004**, *5*, 1181−1186.
(9) Kobayashi, J.; Asahi, T.; Ichiki, M.; Okikawa, A.; Suzuki, H.; Watanabe, T.; Fukada, E.; Shikinami, Y. *J. Appl. Phys*. **1995**, *77*, 2957−2973.
(10) Hoogsteen, W.; Postema, A. R.; Pennings, A. J.; ten Brinke, G.; Zugenmaier, P. *Macromolecules* **1990**, *23*, 634−642.
(11) Tashiro, K.; Sasaki, S.; Kobayashi, M. *Macromolecules* **1996**, *29*, 7460−7469.
(12) Kalb, B.; Pennings, A. J. *Polymer* **1980**, *21*, 607−612.
(13) Puiggali, J.; Ikada, Y.; Tsuji, H.; Cartier, L.; Okinara, T.; Lotz, B. *Polymer* **2000**, *41*, 8921−8930.
(14) Cartier, L.; Okihara, T.; Ikada, Y.; Tsuji, H.; Puiggali, J.; Lotz, B. *Polymer* **2000**, *41*, 8909−8919.
(15) Tsuji, H. *Polymer* **2002**, *43*, 1789−1796.
(16) Metzger, S.; Lippert, B. *J. Am. Chem. Soc*. **1996**, *118*, 12467−12468.
(17) Sigel, R. K. O.; Freisinger, E.; Metzger, S.; Lippert, B. *J. Am. Chem. Soc*. **1998**, *120*, 12000−12007.
(18) Derewenda, Z. S.; Lee, L.; Derewenda, U. *J. Mol. Biol*. **1995**, *252*, 248−262.
(19) Bella, J.; Berman, H. M. *J. Mol. Biol*. **1996**, *264*, 734−742.
(20) Musah, R. A.; Jensen, G. M.; Rosenfeld, R. J.; McRee, D. E.; Goodin, D. B.; Bunte, S. W. *J. Am. Chem. Soc.* **1997**, *119*, 9083−9084.
(21) Steiner, T.; Saenger, W. *J. Am. Chem. Soc*. **1993**, *115*, 4540−4547.
(22) Wahl, M. C.; Sundaralingam, M. *Trends Biochem. Sci.* **1997**, 22, 97−102.
(23) Jeffrey, G. A.; Saenger, W. *Hydrogen Bonding in Biological Structures*; Springer-Verlag: Berlin, 1991.
(24) Scheiner, S. *Hydrogen Bonding: A Theoretical Perspective*; Oxford University Press: New York, 1997.
(25) Hobza, P.; Havlas, Z. *Chem. Rev*. **2000**, *100*, 4253−4264.
(26) Matsuura, H.; Yoshida, H.; Hieda, M.; Yamanaka, S.; Harada, T.; Shin-ya, K.; Ohno, K. *J. Am. Chem. Soc.* **2003**, *125*, 13910−13911.
(27) Desiraju, G. R.; Steiner, T. *The Weak Hydrogen Bond*; Oxford University Press: New York, 1999.
(28) Zhang, J. M.; Tsuji, H.; Noda, I.; Ozaki, Y. *J. Phys. Chem. B* **2004**, *108*, 11514−11520.
(29) Zhang, J. M.; Tsuji, H.; Noda, I.; Ozaki, Y. *Macromolecules* **2004**, *37*, 6433−6439.
(30) Tsuji, H.; Ikada, Y. *Polymer* **1999**, *40*, 6699−6708.
(31) Kister, G.; Cassanas, G.; Vert, M. *Polymer* **1998**, *39*, 267−273.
(32) Qiu, D.; Kean, R. T. *Appl. Spectrosc.* **1998**, *52*, 488−495.
(33) Kang, S.; Hsu, S. L.; Stidham, H. D.; Smith, P. B.; Leugers, M. A.; Yang, X. *Macromolecules* **2001**, *34*, 4542−4548.
(34) Noda, I. *Appl. Spectrosc*. **1993**, *47*, 1329−1336.
(35) Noda, I.; Ozaki, Y. *Two-Dimensional Correlation Spectraoscopy*; John Wiley & Sons: Chichester, U.K., 2004.
(36) Bourque, H.; Laurin, I.; Pézolet, M.; Klass, J. M.; Lennox, R. B.; Brown, G. R. *Langmuir* **2001**, *17*, 5842−5849.

(37) Czarnecki, M. A. *Appl. Spectrosc.* **2000**, *52*, 1583−1590.
(38) Gericke, A.; Gadaleta, S. J.; Brauner, J. W.; Mendelsohn, R.*Biospectroscopy* **1996**, *2*, 341−351.
(39) Lagaron, J. M. *Macromol. Symp*. **2002**, *184*, 19−36.
(40) Schuster, P.; Zundel, G. *The hydrogen Bond: Recent Developments in Theory and Experiments*; North-Holland: Amsterdam, 1976.
(41) Sutor, D. J. *Nature* **1962**, *195*, 68−69.
(42) Taylor, R.; Kennard, O. *J. Am. Chem. Soc*. **1982**, *104*, 5063−5070.
(43) Steiner, T.; Saenger, W. *J. Am. Chem. Soc.* **1992**, *114*, 10146−10154.
(44) Rozenber, M.; Loewenschuss, A.; Marcus, Y. *Phys. Chem. Chem. Phys.* **2000**, *2*, 2699−2702.
(45) Tretinnikow, O. N.; Kato, K.; Iwata, H. *Langmuir* **2004**, *20*, 6748−6753.

MA047872W